

Individual Detection and Characterization of Non-Electrocatalytic, Redox-Inactive Particles in Solution via Electrochemistry

E. Laborda^{*,a}, A. Molina^a, C. Batchelor-McAuley^b, R.G. Compton^b

^a *Departamento de Química Física, Facultad de Química, Regional Campus of International Excellence "Campus Mare Nostrum", Universidad de Murcia, 30100 Murcia, Spain*

^b *Department of Chemistry, Physical & Theoretical Chemistry Laboratory, Oxford University, South Parks Road, Oxford OX1 3QZ (UK). Fax: (+44) 1865-275-410*

* Corresponding author:

Tel: +34 868 88 7433

Fax: +34 868 88 4148

Email: elaborda@um.es

Abstract

The fundamentals and recent examples of applications of electrochemical techniques to the study of *individual* entities in solution are overviewed. Specifically, strategies that enable rapid and simple investigation of redox-inactive and non-catalytic particles are highlighted, broadening the range of entities that can be examined and so the value and capabilities of electrochemistry in the field.

Keywords: impact electrochemical methods; soft nanoparticles; blocking events; liquid|liquid interfaces; capacitive events

1. Background

The use of conventional electrochemical measurements for the characterization and tracking of synthetic and natural micro- and nano-particles has greatly developed in the last decade. Particle properties and their behaviour are a function of their size, shape, composition, state of aggregation, concentration, surface charge, redox activity, etc. and they all can be investigated via electrochemistry in a simple, inexpensive and rapid way ^[1-6]. Moreover, the results obtained are highly representative since the measurements can be performed *in situ* in solution and particle-by-particle, in contrast with other methods that require vacuum conditions (*eg.*, electron microscopies) or that have an ensemble-averaging nature (*eg.*, dynamic light scattering).

1.1. Overview of strategies and types of events

Excellent and comprehensive reviews of the state-of-the-art are available, with special attention being paid to both direct (the particle itself is either electro-oxidized or reduced) and mediated (the particle catalyses the electrode reaction of a redox active couple in the solution phase) Faradaic impacts ^[1]. Another electrochemical strategy for the detection of individual conducting particles include the ‘area amplification’ approach^[7], where the particle collision

leads to a significant increase of the electroactive area of an electrode of comparable dimensions with the consequent increase in the current signal, and the 'open circuit potential' approach ^[8], where the 'mixed potential' of the electrode when no current flows shifts upon the particle arrival at the electrode surface reflecting the different electron transfer kinetics at the microelectrode and the nanoparticle materials.

Impact experiments are generally performed making use of a high-sensitivity trans-impedance amplifier and a conventional three-electrode set-up placed in a Faraday cage where a microelectrode acts as the working electrode. The particle suspension is injected in the electrolyte solution of the electrochemical cell where the potential of the working electrode is set at an appropriate value so that the current-time response reveals the collision of particles at the microelectrode surface in different ways (see Scheme 1). The value of the electrode potential is chosen attending to the particular mechanism of detection; thus, for example, for the study of metallic nanoparticles via direct Faradaic impacts, the electrode potential must be positive enough with respect to the formal potential of oxidation of the metal in the corresponding nanoparticulate form in order to electrolyse the particle.

The methods above-mentioned are suitable for the investigation of redox (by itself ^[9], its content ^[10] or a redox label ^[11]), electrocatalytic ^{[12][8]} or conducting ^[7] particles. In order to complement these works, this Review will highlight simple, electrochemical strategies that enable the study of redox-inactive, non-electrocatalytic and non-conducting particles (such as cells, bacteria, viruses, liposomes, vesicles, emulsion droplets, hydrogels, micro-reactors and drug delivery carriers) without introducing redox labels.

The detection of individual particles in the methods considered is inferred from the appearance of sudden, discrete drops or rises of the otherwise smooth current-time signal at an electrode or liquid|liquid interface, often of micrometric size, held under potentiostatic control. Under appropriate conditions, each distortion arises as a consequence of the arrival of a single particle at the 'sensing area'. The particle may arrive by virtue of their Brownian

motion and, sometimes, the mass transport is enhanced by external directed forces such as controlled convection, magnetic and electric fields. Noting the underlying physicochemical process behind such ‘signal events’, the different techniques here considered will be classified as follows:

- I. *Blocking events* (Section 2): the particle partially obstructs the electric current in the circuit by hindering either the limiting electrode reaction (a) or the flow of ions between the electrodes (b)
 - a. *Blocking the electrode reaction* (Scheme 1)
 - b. *Blocking the ionic current flow* (resistive pulse sensing) (Scheme 2)
- II. *Events at interfaces between two immiscible liquid electrolytes (ITIES)* (Section 3 and Scheme 3): the collision of the particle takes place at a polarized liquid|liquid interface and it triggers a charge transfer reaction
- III. *Capacitive events* (Section 4 and Scheme 4): the impact of the particle perturbs the electrical double layer of the electrode|solution interface giving rise to current events of non-Faradaic nature (*i.e.*, no charge is transferred across the interface)

An additional category could be defined and referred to as ‘bridging impacts’ as in very recent experiments by Compton *et al.* ^[13,14] where carbon nanotubes are detected individually when landing on the sensor in such a way that they bridge a micron-sized gap between two microbands of an interdigitated electrode. From the magnitude of the resulting current increase, the resistance of the nanotube-electrode contact can be determined.

1.2. Types of events and limit of detection

In general, different types of ‘events’ in the current-time response can be observed depending on the persistence of the alteration of the conditions near the sensing area in terms of charge transfer kinetics, distribution of electroactive species, supporting electrolyte ions and electric potential, and/or accessibility to the electrode surface. When the interface does not

recover the original conditions after the particle collision, *step-like* current transients are observed; this can correspond to the irreversible adhesion of the particle to the sensing zone as frequently encountered in methods based on the blocking of an electrode reaction (Scheme 1). Conversely, when the interaction of the particle with the sensing zone is temporary or when the particle vanishes upon collision, *spike-like* (Schemes 2 and 3) or *pulse-like* (Scheme 2) events are recorded. Going into further detail, ‘secondary’ features can be identified in the morphology of the current events, which have been ascribed to a variety of phenomena such as multiple collisions of one particle ^[15], surface rearrangements after collision ^[16,17], particle rotation ^[18], interactions between the surface charges of particles and sensing zone ^[19], Marangoni effects ^[20] and charge transfer kinetics ^[21].

The goal in this kind of electrochemical experiment is collecting hundreds or even thousands of collisions from which distribution properties of the particles can be derived. In order to achieve this aim with good signal resolution and in an acceptable amount of time, suitable experimental conditions must be assured ^[1]. This implies appropriate selection of mass transport conditions, geometry of the sensor and instrumentation.

Given the small magnitude of the signals, ‘sensing areas’ of very small size are employed to enhance the signal-to-noise and signal-to-background ratios ^[22,23]. Thus, ultramicroelectrodes (UMEs), nanopores and nanopipettes and liquid|liquid microinterfaces are employed. However, the reduction of the sensing area makes the probability of observing an event lower ^[24]; consequently, ‘pre-concentration’ mechanisms may be necessary to constrain the duration of the experiments to a few minutes. Thus, under diffusion only conditions particle concentrations in the pM-range are typically employed. This *practical* limit of detection has been lowered by accelerating the particle collection through electromigration in the case of charged particles (up to fM concentration levels ^[16] using low-supported media), controlled convection ^[25,26], magnetic fields ^[27–31], electric fields ^[16,32,33], arrays of UMEs ^[34–37],

as well as combined strategies ^[31,36] through which sub-aM concentrations have been reached ^[31].

1.3. Theoretical modelling and quantitative analysis

Information about the characteristics of the particle can be gained mainly from the features of the events (magnitude, shape and duration) and from their frequency. The former requires understanding the mechanism for each type of collision, and they will be overviewed in Sections 2-4. It is noted that when the duration of the current spikes is very short and the signal is very small, special caution must be taken with regard to distortions imposed by the bandwidth of the recording electronics ^[38]; thus, for typical values of 10-20 kHz, events shorter than 100 μ s can be severely attenuated or even vanished. Overcoming this limitation involves the development of high-performance instrumentation that allow for low-noise measurements at very high bandwidth, as well as strategies to enhance the magnitude and/or extend the duration of the events; for example, in resistive pulse sensing the pore walls can be modified to make the particle translocation longer (Section 2.2).

Regarding the event frequency, its value is related to the operating mass transport mechanism(s) in solution. In the absence of forced convection and magnetic fields, the most determining mechanism (either diffusion or migration) can be identified and tuned through the concentration of supporting electrolyte: the smaller the migrational contribution, the smaller the effect of the electrolyte concentration on the impact frequency. Also note that this aspect is important when analysing the property distributions obtained electrochemically that can be biased towards certain particles. For example, when diffusion predominates, the collision frequency of smaller particles with faster diffusivity will be higher (Eqs. (1)) such that the distribution data will emphasize them; analogously, in case that migration dominates, the number of particles with higher electrophoretic mobility (*i.e.*, higher charge) will be 'overweighed'.

In the simplest situation where particles reach the sensing area only by diffusion, the following simple expressions relate the frequency of impacts (f^{diff}) to the concentration of particles (c_{NP}) and to the particle's diffusion coefficient (D_{NP} , from which the particle size can be inferred) when disc, hemispherical or cylindrical UMEs are employed ^[1]:

$$\begin{aligned}
 f_{disc}^{diff} &= 4D_{NP}c_{NP}r_{disc}N_A \\
 f_{hemi}^{diff} &= 2\pi D_{NP}c_{NP}r_{hemi}N_A \\
 f_{wire}^{diff} &= \pi D_{NP}c_{NP}lN_A \left(\frac{r_{wire}}{\sqrt{\pi Dt}} e^{-0.1 \frac{\sqrt{\pi Dt}}{r_{wire}}} + \frac{1}{\ln \left(5.2945 + 1.4986 \frac{\sqrt{Dt}}{r_{wire}} \right)} \right)
 \end{aligned} \tag{1}$$

where r is the radius of the disc, hemisphere or wire, l is the length of the wire and N_A is the Avogadro constant. If migration dominates (for example, with 'large' particles and/or with low concentration of supporting electrolyte), a ballpark estimate of the event frequency can be obtained from the following approximate expression derived with simple transference number considerations without including the contribution of the ions generated by the electrode reaction ^[33]:

$$f^{mig} \approx \frac{t_{NP}}{z_{NP}F} I \tag{2}$$

where t_{NP} is the transference number of the particle ^[39], z_{NP} is its charge number, F is the Faraday constant, and I the current flowing through the circuit. Although the above expressions may enable the tentative evaluation of the key mass transport mechanism, accurate analysis of the event frequency is likely more complex attending to the number of factors that affect its value (generally by decreasing it): near-wall hindered diffusion (especially as the size ratio of particle-to-electrode increases) ^[40–42], particle adsorption at the insulating shielding of the UME ^[43], contamination of the sensing area ^[44], particle agglomeration,... Prior calibration can be considered in those cases where appropriate standards are available, noting

that the results are not merely dependent on the particle size but also on other particle features as discussed below.

2. Blocking events

This group of methods is of very general application so that, in principle, particles of any nature can be detected. For the same reason, these approaches lack selectivity unless ‘indirect strategies’ are used to gain information on the nature of the particles, such as via the chemical modification/functionalization of the sensing area ^[45] or of the particles ^[46].

For the signal events to be measurable, a significant area/volume of the current flow path must be obstructed by the particle so that the use of small sensing areas is particularly important in this case. Thus, the study of ‘true’ nanoparticles (<100 nm) has only been possible after the emergence of submicrometric electrodes and nanopores/pipettes.

2.1. Blocking the electrode reaction

In contrast to electrocatalytic amplification ^[12], in these methods the detection of the particles is based on the hindrance of an ongoing electrode reaction ^[47] (A-to-B in Scheme 1) and hence the less of electrochemical signal. Since Lemay’s seminal work ^[32], the rationale and fundamentals have been well-established via combined electrochemical and optical monitoring of insulating microbeads of different materials ^[16,32,47]. It was demonstrated that the electrochemical events observed were associated with particles landing on the UME active area (blocking a portion of the electrode surface) or close to it (perturbing the mass transfer field ^[16,17,23]).

As a rule of thumb, for events to be measurable the size of the UME must not be much more than one order of magnitude larger than the particles under study ^[16,48,49]. Thus, with conventional microelectrodes (*ca.* 1-30 μm) this methodology has been applied to the study of entities of size between a few microns and hundreds of nanometers, including oil-in-water ^[50] and water-in-oil ^[51] emulsion droplets, viruses ^[46], vesicles ^[52], bacteria ^[49] and self-propelled

micromotors ^[53]. With submicrometric electrodes (*ca.* <300 nm in diameter), the detection of single biomacromolecules of a few nanometers (enzymes, antibodies and DNA) has been achieved ^[48].

With regard to the shape of the events, step-like ones are the most frequently recorded, except for a few examples where spike-like transients have been obtained when the particle only distorts the diffusion layer or its adhesion to the UME surface is not permanent as in the studies of self-propelled micromotors ^[53] and particles in microfluidic systems ^[31].

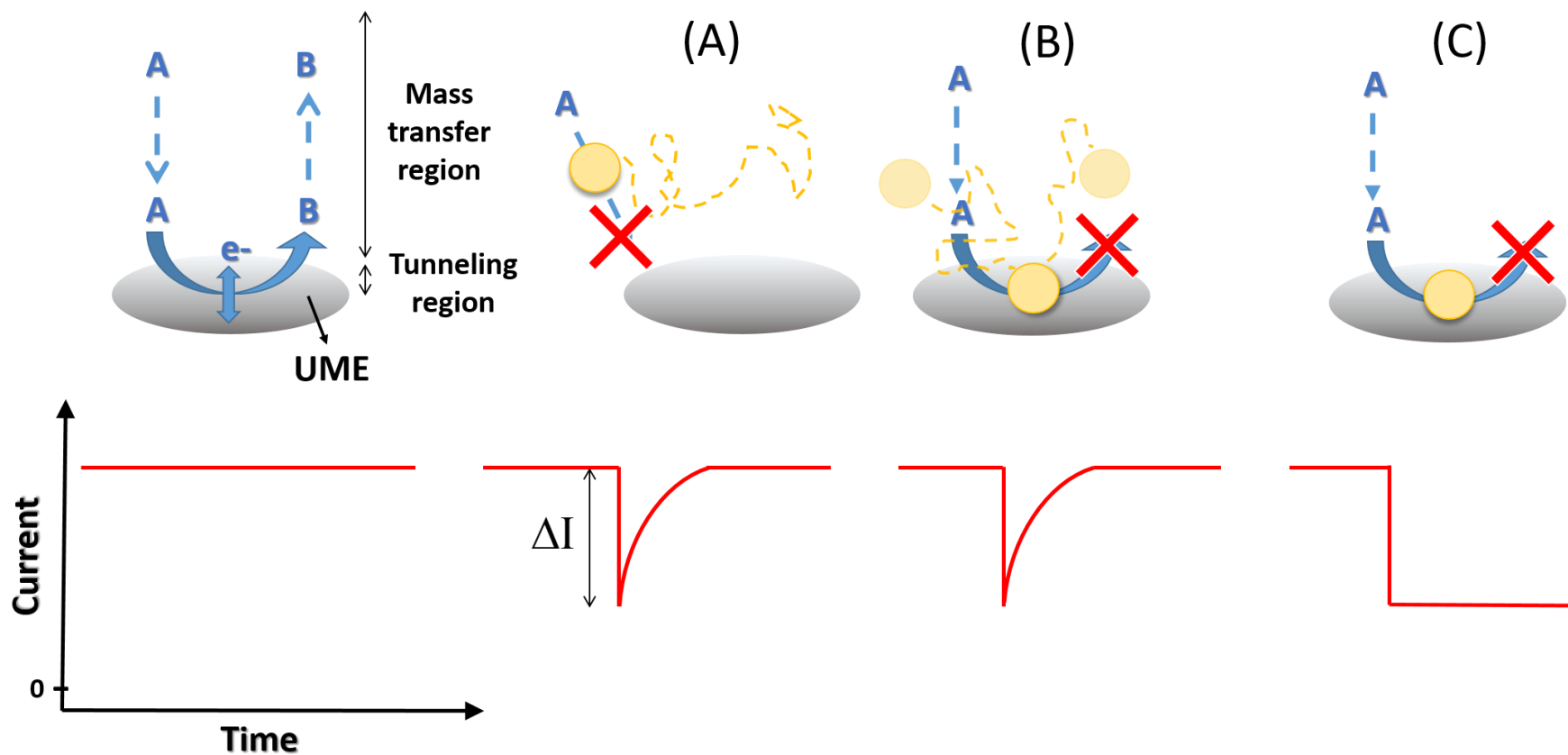
The magnitude of the steps allows for the quantification of the particle size. Typically, UMEs of disc geometry are employed for the measurements, with the magnitude of the events (ΔI , see Scheme 2) depending on the position of the particle landing. This is a consequence of the non-uniform flux of electroactive species over the disc surface, increasing from the centre to the edge; hence, the closer to the edge the impact takes place, the larger the blocking effect of the impact on the current signal. Approximate expressions for ΔI in the case of totally impermeable to the redox moiety have been proposed, by simplifying the 3-dimensional problem of the successive landing of particles to a 2-dimensional problem of individual, perfectly-spherical particles landing on a bare microdisc ^[16]:

$$\Delta I_{sph} \approx I_{disc} \left(\frac{r_{NP}}{r_{disc}} \right)^2 f_{landing} \quad (3)$$

where $f_{landing}$ is a geometric factor dependent on the landing position; thus, at the edge of a microdisc (where the particle landing is more probable attending to geometric and electrostatic considerations ^[17]) $f_{landing}$ takes the value of 0.574 ^[23]. I_{disc} is the current at the UME, which is proportional to the concentration of redox species. Thus, noting Eq. (3) it can be concluded that the magnitude of the signal blockage can be enhanced by reducing the size of the UME and also by increasing the concentration of electroactive species ^[46,49] provided that this is compatible with the sample and with the solubility of the redox probe ^[16].

The dependence of the magnitude of the events on the landing position at microdiscs introduces complexity in the modelling, and uncertainty in the interpretation of experimental data. The use of hemispherical or cylindrical electrodes where the flux of redox species is uniform over their surface ^[39,54,55] are likely helpful, or alternatively, the event frequency could be used to extract the particle size distribution with the necessary caveats mentioned in Section 1.

Scheme 1 – Schematic of the different situations and event morphologies that can be recorded in blocking impacts experiments depending on whether the particle affects *temporary* the mass transfer of electroactive reagent (**A**) and/or the electron transfer event (**B**), or the particle sticks to the electrode surface and blocks *permanently* a portion of the electrode active area (**C**). UME = ultramicroelectrode ^[31,50]



2.2. Blocking an ionic current flow: resistive-pulse sensing

In this category we include the well-known and developed resistive-pulse sensing techniques ^[45,56–58]. Coulter counters have long been employed for the detection of micrometer sized particles, the contraction of the sensing pore size has enabled the detection of far smaller species even allowing single molecule detection ^[45,56–58]. The sensing strategy is based on monitoring an ionic current across an orifice, upon translocation of a particle from one compartment to another a drop in the electric current is observed (see Scheme 2). This drop in current occurs due to the displacement by the particle of a significant volume of the electrolyte solution that is, in general, more conductive than the particle. (Perhaps worth a comment that high electrolyte concentrations are generally not compatible with colloidal solutions? This is a problem for many impact type experiments but especially an issue here. The q-nano is a commercial device based on this technology) While continuing advances in the fabrication and characterization of nanopores and nanopipettes ^[57] of extremely small volume allow for the investigation of nanometric entities ^[45,57,59–63]. It is also important to highlight the value of tuneable-size pores that enable *ad hoc* and real-time tuning of the orifice size for wider size detection range and higher sensitivity. Also, multifunctional nanopipettes that combine resistive pulse sensing with electrocatalytic ^[59] and blocking ^[64] collision measurements have been developed.

The shape of the events recorded depends mainly on the geometry of the channel since this affects the spatial distribution of the electric field ^[65–67]. Channels are mostly either cylindrical or conical with the latter offering lower detection limits as well as information about the direction of the translocation (see Scheme 2) for the confinement of most of the electric field near the smaller opening of the pore ^[66,67]. As shown in Scheme 2, pulse-like events are observed at cylindrical pores and spike-like ones at conical pores. Also, staircase steps have been observed when the interaction between the particle and the pore/pipette wall is strong and so irreversible adhesion takes place ^[68,69]. The precise shape and height of the event is

affected by additional factors such as the surface charge on the particle and on the pore walls [19,70], the particle deformability and conductance (hydrogel particles [71]), the rotation of anisotropic particles [18], the entrance trajectory of the particle [72],...

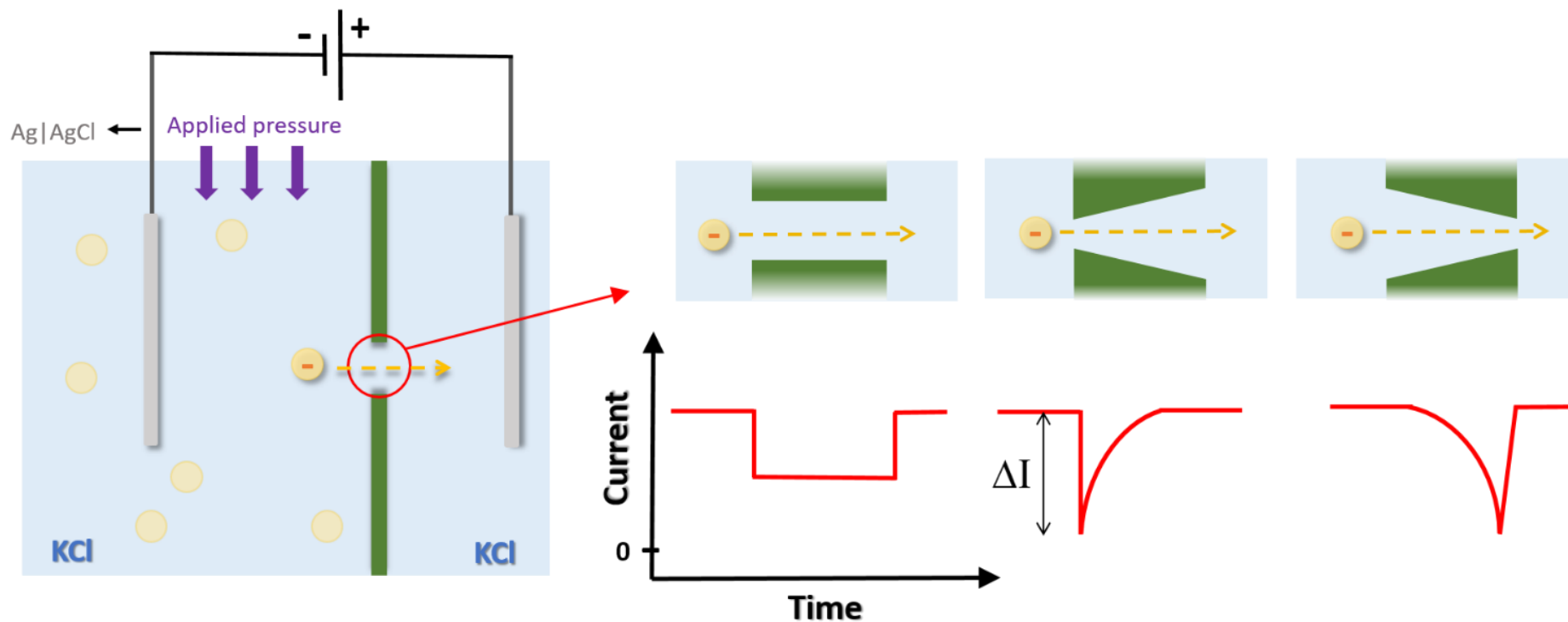
Regarding the magnitude of the current decrease during the event (ΔI), this depends on the particle shape and the pore geometry. Approximate expressions have been derived that relate ΔI with the particle volume; for example, for the translocation of spherical particles through a cylindrical channel at a constant applied voltage it is obtained that [45,57,73,74]:

$$\Delta I_{sph} \approx I_{baseline} \frac{d_{NP}^3}{\left(l_{pore} + \frac{\pi}{4} d_{pore}\right) d_{pore}^2} f(d_{pore}, d_{NP}) \quad (4)$$

where $f(d_{pore}, d_{NP})$ is a correction factor that depends on the nanoparticle-to-nanochannel diameter ratio ($f(d_{pore}, d_{NP}) \approx 1 / (1 - 0.8 d_{pore}^3 / d_{NP}^3)$ for $d_{pore} / d_{NP} < 0.8$ [73]). On the basis of Eq. (4), the signal has (roughly) a cubic dependence on the particle radius such that these techniques show a high ability to discriminate particles of different size, with sub-nanometer resolution having been achieved [63].

Finally, the duration of the events as a result of the translocation dynamics of the particle can be controlled for a given particle-pore system through the channel geometry, the applied voltage, the applied pressure and the electrolyte concentration; these factors determine the interplay between the diffusional, electric, frictional and hydrodynamic forces acting on the particles [75]. As the diameter of the pore/pipette shrinks, the electrophoretic and electroosmotic forces become more important and, under conditions where the former dominates, the surface charge and concentration of the particles can be estimated from the duration and frequency of the events as determined by their electrophoretic mobility. Note that the possibility of controlling the length of the events is also very convenient to reduce distortions associated with limitations of the instrumentation (see Section 1).

Scheme 2 - (left) Schematic of the resistive-pulse analysis of nanoparticles with their translocation being driven/controlled via voltage and pressure gradients; (right) Typical current-time events corresponding to the translocation of a single nanoparticle depending on the shape of the pore and the translocation direction. [18,19]



3. Events at ITIES

The suitability of ion transfer processes across externally polarized ITIES (interfaces between two immiscible liquid electrolytes) for the electrochemical detection of individual particles has been recently assessed ^[76], noting the advantages that such soft interfaces can offer (reproducibility, absence of defects, mechanical flexibility, easy-to-modify) as well as to their interest as biomimetic platforms.

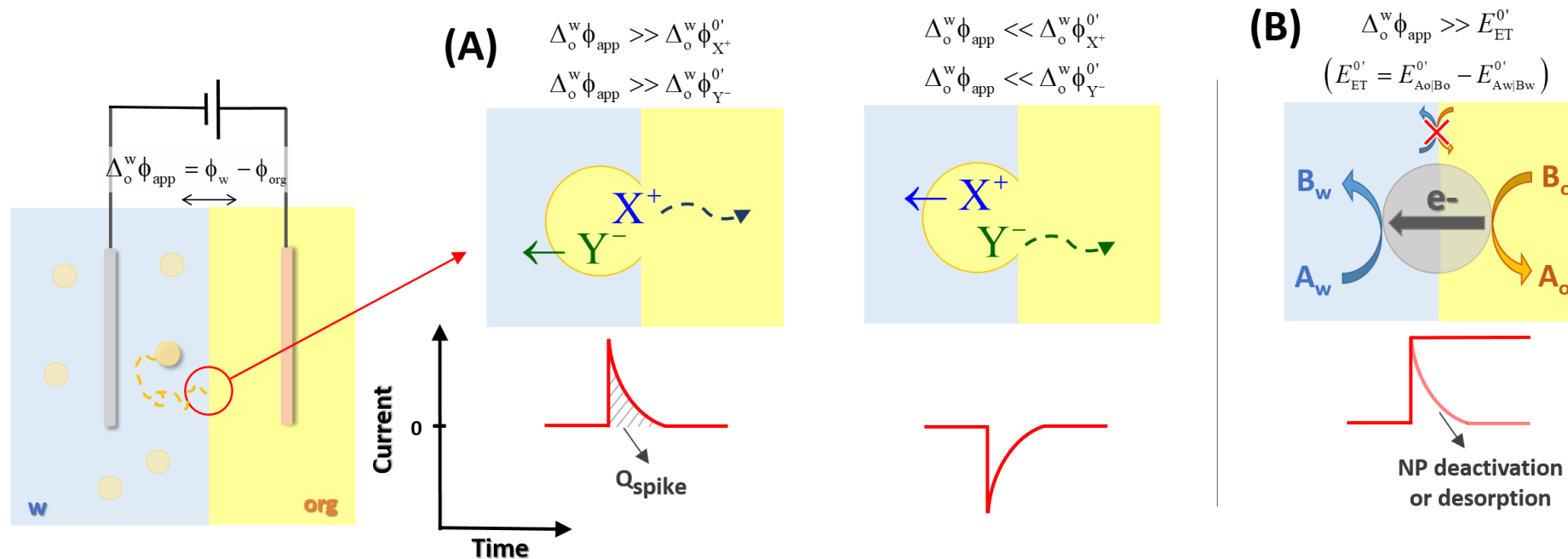
With the first methodology of this type recently-introduced ^[76], soft particles containing some ionic load (for example, as it is commonly the case of cells and organelles) can be detected and examined. As shown in Scheme 3A, the underlying process for detection is the *selective* and quantitative interfacial transfer of one of the ions released upon the collision and fusion of the particle with the interface. This is achieved by polarizing conveniently the liquid|liquid interface, with a 2- ^[77,78] or 4- ^[79,80] electrode set-up and an external power supply, attending to the transfer Gibbs energy of the different ionic species. As a result, a net charge transfer between the two phases takes place in each collision and a spike on the current-time response is obtained. From the value of the charge under the spike (Q_{spike} , which is highly unaffected by bandwidth issues ^[38]), the size of the particles or the concentration of their ionic load can be determined; for example, for spherical particles (such as emulsion droplets) the following cubic relationship can be established between Q_{spike} and the particle diameter (d_{NP}):

$$Q_{\text{spike}} = \frac{1}{6} \pi F z_i c_i d_{\text{NP}}^3 \quad (5)$$

where z_i and c_i are the charge number and the concentration inside the particle of the transferred ion i ; note that the sign of the charge informs about whether a cation or an anion is transferred across the interface (see Scheme 3A). Also note that the dependence of Q_{spike} on the applied Galvani potential difference provides selectivity to this method such that information can be gained on the nature of the content of the particles.

Also, based on the studies of ensembles of metallic nanoparticles adsorbed at ITIES ^[81–83], the feasibility of their individual detection by using microinterfaces has been proven very recently ^[20]. For this, an electrocatalytic amplification approach has been followed such that a biphasic electron transfer reaction is mediated by the particle as it collides and adsorbs at the interface, acting as a bipolar nanoelectrode (see Scheme 3B).

Scheme 3 - Schematic of the main strategies developed for the detection of micro- and nano-particles with externally polarized liquid|liquid interfaces: **(A)** the particle load acts as a finite reservoir of transferable ions and, due to their depletion, spike-like events are observed; **(B)** the particle adsorbs at the soft interface and it mediates a biphasic redox reaction acting as a bipolar nanoelectrode such that a step-like event can be predicted unless particle deactivation or desorption takes place. $\Delta_o^w \phi_{app} (= \phi_w - \phi_{org})$ = interfacial Galvani potential difference; $\Delta_o^w \phi_i^{0'}$ = formal transfer potential of species i . [20,76,83]



4. Capacitive events

The distortion of the electrode-solution charge balance at the electrical double layer (EDL) at the working electrode|solution by particles in solution has been demonstrated to give rise to measurable current-time events recorded with mercury electrodes and solid microelectrodes ^[84–92]. The events are spike-shaped, similar to those observed in some Faradaic impact experiments, though they show a ‘peculiar’ potential-dependence that enables identification. Thus, while Faradaic impacts due to a single redox reaction appear at potentials more positive (if it is an electro-oxidation) or more negative (in the case of an electro-reduction) than a ‘threshold potential’ (related to the formal potential and rate of the redox process) and they always have the same sign, the sign of capacitive spikes switches at a certain inversion potential that have been related to the potential of zero charge ^[87] and to the electronic properties/capacitance of the particles ^[86,88] (see Scheme 4).

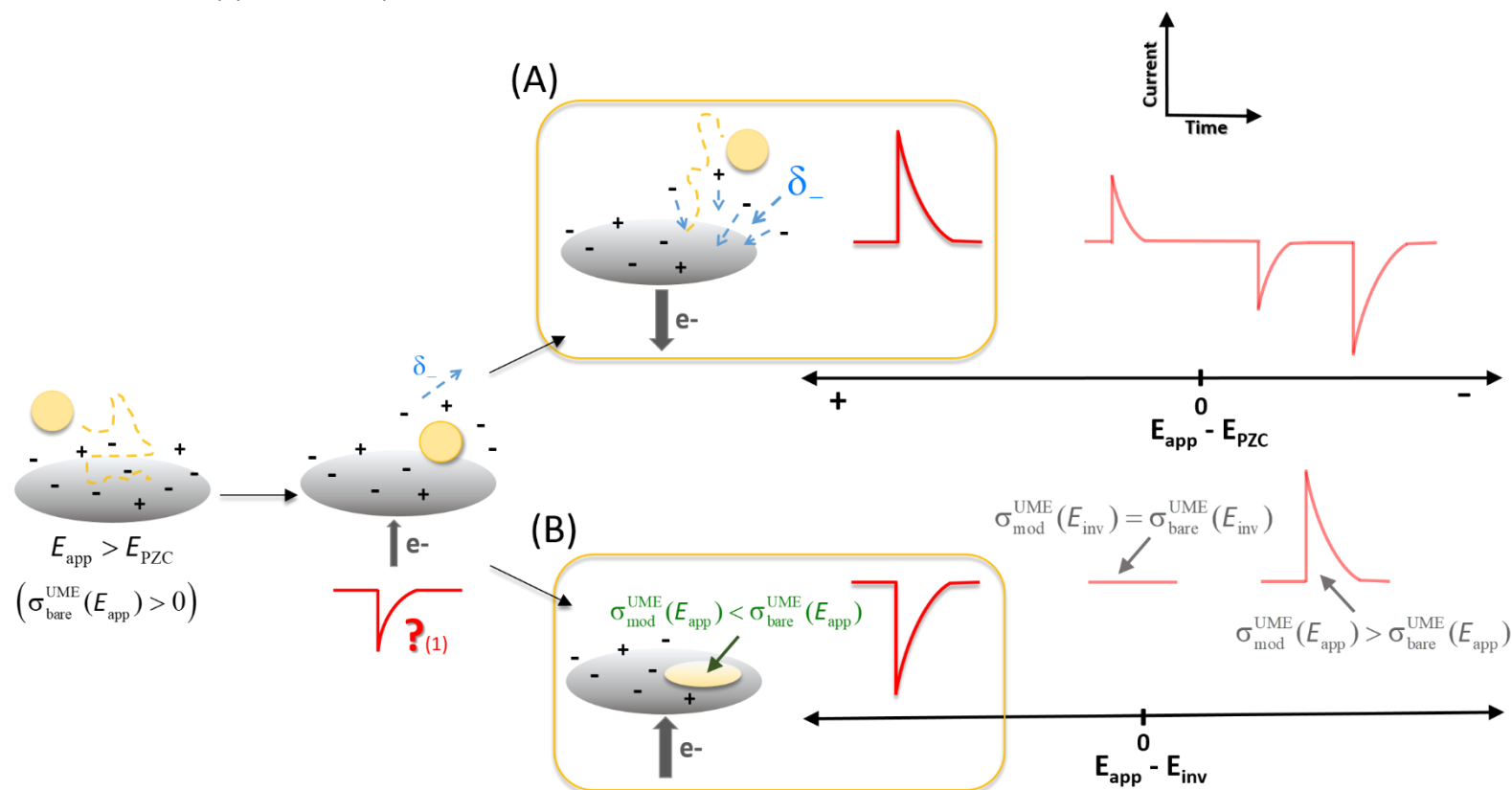
On the basis of the above evidence, the origin of this type of events has been associated with the perturbation of a portion of the EDL by the colliding particle with the subsequent charging-discharging processes. Different microscopic scenarios have been proposed assuming either a temporary approach of the particles to the electrode|solution interface (based on experimental results with alumina, graphite and copper particles ^[87] and graphene platelets ^[88]) or a permanent adhesion to the electrode surface (based on experiments with droplets, liposomes and montmorillonite particles ^[85,86,90]). Thus, an electron flow will take place to adjust conveniently the local excess charge density on the electrode side as a consequence of the perturbation provoked by the impacting particle via transient exclusion of ions from the double layer (Scheme 4A), or via permanent modification of a portion of the interface affecting its double layer features (Scheme 4B).

Detection methodologies based capacitive impacts are very convenient since they can be applied to particles of any nature and without addition of either redox probes in solution (Section 2.1) or ionic markers (Section 3). Nevertheless, given that the charge involved is

generally very small, the detection of nanoparticles is particularly challenging and particles of micrometric size (at least in one dimension), which can affect relatively 'large' areas of the EDL, have been mostly reported. An exception worth noting is the line under development by Lemay and co-workers ^[37] through which the detection of individual landing nanoparticles has been achieved by recording changes in capacitance with time of sensors surfaces composed of thousands of nanoelectrodes of highly-reduced parasitic noise.

Scheme 4 - Schematic of the mechanisms proposed to justify the features of capacitive spikes relying on the perturbation of the charge distribution at the electrical double layer and/or on the adhesion of the particle creating a new electrode|particle interface that show different capacity and charge density than the original interface. E_{PZC} = potential of zero charge; σ_{bare}^{UME} = potential-dependent surface charge density on the bare electrode; σ_{mod}^{UME} = potential-dependent surface charge density on the electrode as modified by the nanoparticle material; E_{app} = potential applied at the ultramicroelectrode. [85,87,90] (1)

The experimental capacitive impacts reported are unidirectional at a given applied potential, which may call into question the ability (time response) of the instrumentation to record all the 'history' of the event, which could imply bidirectional spikes under certain conditions.



5. Summary and Outlook

In the era of nanoscience and nanotechnologies, electrochemical methods have greatly developed in recent years towards the investigation of single micro/nano-particles in solution. Among them, those devoted to 'hard' conducting particles have progressed intensively, with successful application to a variety of materials, particularly, metallic, carbon and semiconductor nanoparticles.

Electrochemical methods for the individual study of so-called 'soft' particles (cells, emulsion droplets, viruses, vesicles, liposomes) have also achieved promising outcomes for particle detection and characterization in solution, in a few minutes and with simple and relatively economical instrumentation. Within this context, several strategies can be found based on the alteration of the electrochemical signal as a result of the collision of the particle with a (sub)micrometric electrode|liquid or liquid|liquid interface. The signal distortion ('event') can result from the blocking of an ongoing electronic or ionic current, the release of a load of transferable ions next to a polarized liquid|liquid interface, or the transient disruption of the electrode-solution charge balance at the electrical double layer. Generally speaking, the magnitude of the event can be related (though not always in a simple way) to the size and aggregation state of the particles, and the impact frequency to the particle concentration.

Progress in the field will certainly involve further development of stochastic-deterministic models that articulate the understanding of these complex systems, ideally through simple analytical expressions, and allow for calibration-less analysis of experimental data. Among others, accurate theoretical treatments for non-spherical particles would be convenient as well as for impact experiments in media of low ionic strength considering that such conditions can be useful to minimize particle aggregation or to ensure the stability of biological samples. Moreover, it will be worth deriving theoretical tools that enable the characterization of the dynamics of the underlying physicochemical processes from the shape and duration of the transients in the different strategies. This can greatly benefit from the

combination of electrochemical, optical and spectroscopic techniques in impact experiments, as well as from advanced instrumentation with very short time response and high sensitivity to avoid contrived effects by the circuitry.

The design of optimized platforms for very small interfaces in a level where nanometric and even molecular entities can be tracked online and real time will find applications in biomedicine (*eg.*, assessment of drug delivery systems) and environmental monitoring (*eg.*, evaluation of the impact of nanomaterials). Also, the implementation of novel electrochemical strategies can be envisaged. Indeed, the use of liquid|liquid microinterfaces can be broaden considering alternative detection principles such as blocking of an ion transfer process by the particle arrival, changes in the interfacial capacitance or shift of the open circuit potential.

Acknowledgements

EL and AM thank the financial support of the Fundación Séneca de la Región de Murcia (19887/GERM/15) and the MINECO (Spanish government, Project CTQ2015-65243-P and Juan de la Cierva fellowship). RGC and CBM thank the European Research Council for funding under the European Union's Seventh Framework Programme (FP/2007-2013)/ERC Grant Agreement no [320403].

References

- [1] S. V. Sokolov, S. Eloul, E. Kätelhön, C. Batchelor-McAuley, R. G. Compton, *Phys. Chem. Chem. Phys.* **2017**, *19*, 28–43.
- [2] P. H. Robbs, N. V. Rees, *Phys. Chem. Chem. Phys.* **2016**, *18*, 24812–24819.
- [3] M. V. Mirkin, S. Amemiya, *Nanoelectrochemistry*, CRC Press, Boca Raton, **2015**.
- [4] M. Pumera, *ACS Nano* **2014**, *8*, 7555–7558.
- [5] Y.-Y. Peng, R.-C. Qian, M. E. Hafez, Y.-T. Long, *ChemElectroChem* **2017**, *4*, 977–985.
- [6] K. J. Stevenson, K. Tschulik, *Curr. Opin. Electrochem.* **2017**, DOI 10.1016/j.coelec.2017.07.009.
- [7] J. H. Park, S. N. Thorgaard, B. Zhang, A. J. Bard, *J. Am. Chem. Soc.* **2013**, *135*, 5258–5261.
- [8] H. Zhou, J. H. Park, F.-R. F. Fan, A. J. Bard, *J. Am. Chem. Soc.* **2012**, *134*, 13212–13215.
- [9] Y.-G. Zhou, N. V. Rees, R. G. Compton, *Angew. Chemie Int. Ed.* **2011**, *50*, 4219–4221.
- [10] J. E. Dick, *Chem. Commun.* **2016**, *52*, 10906–10909.
- [11] L. Sepunaru, B. J. Plowman, S. V. Sokolov, N. P. Young, R. G. Compton, W. Chen, S. Liu, M. Marappan, X. Zhao, Y. Miao, et al., *Chem. Sci.* **2016**, *7*, 3892–3899.
- [12] X. Xiao, A. J. Bard, *J. Am. Chem. Soc.* **2007**, *129*, 9610–9612.
- [13] X. Li, C. Batchelor-McAuley, L. Shao, S. V. Sokolov, N. P. Young, R. G. Compton, *J. Phys. Chem. Lett.* **2017**, *8*, 507–511.
- [14] A. Krittayavathananon, K. Ngamchuea, X. Li, C. Batchelor-McAuley, E. Kätelhön, K. Chaisiwamongkhon, M. Sawangphruk, R. G. Compton, *J. Phys. Chem. Lett.* **2017**, *8*, 3908–3911.
- [15] J. Ustarroz, M. Kang, E. Bullions, P. R. Unwin, *Chem. Sci.* **2017**, *8*, 1841–1853.
- [16] A. Boika, S. N. Thorgaard, A. J. Bard, *J. Phys. Chem. B* **2013**, *117*, 4371–4380.
- [17] S. E. Fosdick, M. J. Anderson, E. G. Nettleton, R. M. Crooks, *J. Am. Chem. Soc.* **2013**, *135*, 5994–5997.
- [18] Y. Zhang, M. A. Edwards, S. R. German, H. S. White, *J. Phys. Chem. C* **2016**, *120*, 20781–

20788.

- [19] W.-J. Lan, C. Kubeil, J.-W. Xiong, A. Bund, H. S. White, *J. Phys. Chem. C* **2014**, *118*, 2726–2734.
- [20] T. J. Stockmann, L. Angelé, V. Brasiliense, C. Combellas, F. Kanoufi, *Angew. Chemie* **2017**, DOI 10.1002/ange.201707589.
- [21] E. N. Saw, M. Kratz, K. Tschulik, *Nano Res.* **2017**, 1–10.
- [22] J. Yao, K. D. Gillis, *Analyst* **2012**, *137*, 2674.
- [23] J. Bonezzi, A. Boika, *Electrochim. Acta* **2017**, *236*, 252–259.
- [24] L. Höfler, R. E. Gyurcsányi, *Anal. Chim. Acta* **2012**, *722*, 119–126.
- [25] T. M. Alligrant, M. J. Anderson, R. Dasari, K. J. Stevenson, R. M. Crooks, *Langmuir* **2014**, *30*, 13462–13469.
- [26] J. Jiang, X. Huang, L. Wang, *J. Colloid Interface Sci.* **2016**, *467*, 158–164.
- [27] D. A. Robinson, J. J. Yoo, A. D. Castañeda, B. Gu, R. Dasari, R. M. Crooks, K. J. Stevenson, *ACS Nano* **2015**, *9*, 7583–7595.
- [28] K. Ngamchuea, K. Tschulik, R. G. Compton, *Nano Res.* **2015**, *8*, 3293–3306.
- [29] J. J. Yoo, J. Kim, R. M. Crooks, H. Kang, T. Kim, T. Hyeon, D. Jeong, Y. Lee, *Chem. Sci.* **2015**, *6*, 6665–6671.
- [30] G. R. Willmott, M. G. Fisk, J. Eldridge, *Biomicrofluidics* **2013**, *7*, 64106.
- [31] J. J. Yoo, M. J. Anderson, T. M. Alligrant, R. M. Crooks, *Anal. Chem.* **2014**, *86*, 4302–4307.
- [32] B. M. Quinn, P. G. van't Hof, S. G. Lemay, *J. Am. Chem. Soc.* **2004**, *126*, 8360–8361.
- [33] J. H. Park, A. Boika, H. S. Park, H. C. Lee, A. J. Bard, *J. Phys. Chem. C* **2013**, *117*, 6651–6657.
- [34] S. Fletcher, *Electrochem. commun.* **1999**, *1*, 502–512.
- [35] K. J. Krause, A. Yakushenko, B. Wolfrum, *Anal. Chem.* **2015**, *87*, 7321–7325.
- [36] S. V. Sokolov, T. R. Bartlett, P. Fair, S. Fletcher, R. G. Compton, *Anal. Chem.* **2016**, *88*,

8908–8912.

- [37] S. G. Lemay, C. Laborde, C. Renault, A. Cossettini, L. Selmi, F. P. Widdershoven, *Acc. Chem. Res.* **2016**, *49*, 2355–2362.
- [38] E. Kätelhön, E. E. L. Tanner, C. Batchelor-McAuley, R. G. Compton, *Electrochim. Acta* **2016**, *199*, 297–304.
- [39] A. J. Bard, L. R. Faulkner, *Electrochemical Methods: Fundamentals and Applications*, Wiley, New York, **2000**.
- [40] E. Kätelhön, R. G. Compton, *Chem. Sci.* **2014**, *5*, 4592–4598.
- [41] S. V. Sokolov, E. Kätelhön, R. G. Compton, *J. Phys. Chem. C* **2016**, *120*, 10629–10640.
- [42] S. Eloul, E. Kätelhön, R. G. Compton, *Phys. Chem. Chem. Phys.* **2016**, *18*, 26539–26549.
- [43] S. Eloul, R. G. Compton, *ChemElectroChem* **2014**, *1*, 917–924.
- [44] E. Kätelhön, W. Cheng, C. Batchelor-McAuley, K. Tschulik, R. G. Compton, *ChemElectroChem* **2014**, *1*, 1057–1062.
- [45] I. Makra, R. E. Gyurcsányi, *Electrochem. commun.* **2014**, *43*, 55–59.
- [46] J. E. Dick, A. T. Hilterbrand, A. Boika, J. W. Upton, A. J. Bard, *Proc. Natl. Acad. Sci. U. S. A.* **2015**, *112*, 5303–8.
- [47] E. Suraniti, F. Kanoufi, C. Gosse, X. Zhao, R. Dimova, B. Pouligny, N. Sojic, *Anal. Chem.* **2013**, *85*, 8902–8909.
- [48] J. E. Dick, C. Renault, A. J. Bard, *J. Am. Chem. Soc.* **2015**, *137*, 8376–8379.
- [49] J. Y. Lee, B.-K. Kim, M. Kang, J. H. Park, *Sci. Rep.* **2016**, *6*, 30022.
- [50] B.-K. Kim, A. Boika, J. Kim, J. E. Dick, A. J. Bard, *J. Am. Chem. Soc.* **2014**, *136*, 4849–4852.
- [51] N. T. T. Hoang, T. L. T. Ho, J. H. Park, B.-K. Kim, *Electrochim. Acta* **2017**, *245*, 128–132.
- [52] E. Lebègue, C. M. Anderson, J. E. Dick, L. J. Webb, A. J. Bard, *Langmuir* **2015**, *31*, 11734–11739.
- [53] J. G. S. Moo, M. Pumera, *ACS Sensors* **2016**, *1*, 949–957.
- [54] R. G. Compton, C. E. Banks, *Understanding Voltammetry*, Imperial College Press,

London, **2010**.

- [55] A. Molina, J. González, *Pulse Voltammetry in Physical Electrochemistry and Electroanalysis*, Springer International Publishing, Berlin, **2016**.
- [56] D. Kozak, W. Anderson, R. Vogel, M. Trau, *Nano Today* **2011**, 6, 531–545.
- [57] L. Luo, S. R. German, W.-J. Lan, D. A. Holden, T. L. Mega, H. S. White, *Annu. Rev. Anal. Chem.* **2014**, 7, 513–535.
- [58] R. R. Henriquez, T. Ito, L. Sun, R. M. Crooks, *Analyst* **2004**, 129, 478–482.
- [59] K. McKelvey, S. R. German, Y. Zhang, H. S. White, M. A. Edwards, *Curr. Opin. Electrochem.* **2017**, DOI 10.1016/j.coelec.2017.06.006.
- [60] M. A. Edwards, S. R. German, J. E. Dick, A. J. Bard, H. S. White, *ACS Nano* **2015**, 9, 12274–12282.
- [61] A. Sikora, A. G. Shard, C. Minelli, *Langmuir* **2016**, 32, 2216–2224.
- [62] P. Terejášnszky, I. Makra, P. Fürjes, R. E. Gyurcsányi, *Anal. Chem.* **2014**, 86, 4688–4697.
- [63] S. R. German, T. S. Hurd, H. S. White, T. L. Mega, *ACS Nano* **2015**, 9, 7186–7194.
- [64] K. McKelvey, M. A. Edwards, H. S. White, *J. Phys. Chem. Lett.* **2016**, 7, 3920–3924.
- [65] C. Y. Lee, C. Chen, *Microsyst. Technol.* **2017**, 23, 299–304.
- [66] W.-J. Lan, D. A. Holden, B. Zhang, H. S. White, *Anal. Chem.* **2011**, 83, 3840–3847.
- [67] W.-J. Lan, H. S. White, *ACS Nano* **2012**, 6, 1757–1765.
- [68] T. Li, X. He, K. Zhang, K. Wang, P. Yu, L. Mao, A. G. Ewing, G. K. H. Wiberg, S. Ashton, U. Heiz, et al., *Chem. Sci.* **2016**, 7, 6365–6368.
- [69] D. J. Niedzwiecki, J. Grazul, L. Movileanu, *J. Am. Chem. Soc.* **2010**, 132, 10816–10822.
- [70] Y. Qiu, C.-Y. Lin, P. Hinkle, T. S. Plett, C. Yang, J. V. Chacko, M. A. Digman, L.-H. Yeh, J.-P. Hsu, Z. S. Siwy, *ACS Nano* **2016**, 10, 8413–8422.
- [71] M. Pevarnik, M. Schiel, K. Yoshimatsu, I. V. Vlassiouk, J. S. Kwon, K. J. Shea, Z. S. Siwy, *ACS Nano* **2013**, 7, 3720–3728.
- [72] M. Tsutsui, Y. He, K. Yokota, A. Arima, S. Hongo, M. Taniguchi, T. Washio, T. Kawai, *ACS*

Nano **2016**, *10*, 803–809.

- [73] T. Ito, L. Sun, R. R. Henriquez, R. M. Crooks, *Acc. Chem. Res.* **2004**, *37*, 937–945.
- [74] M. Davenport, K. Healy, M. Pevarnik, N. Teslich, S. Cabrini, A. P. Morrison, Z. S. Siwy, S. E. Létant, *ACS Nano* **2012**, *6*, 8366–8380.
- [75] S. R. German, L. Luo, H. S. White, T. L. Mega, *J. Phys. Chem. C* **2013**, *117*, 703–711.
- [76] E. Laborda, A. Molina, V. F. Espín, F. Martínez-Ortiz, J. García de la Torre, R. G. Compton, *Angew. Chemie* **2017**, *129*, 800–803.
- [77] T. Osakai, T. Kakutani, M. Senda, *Bull. Chem. Soc. Jpn.* **1984**, *57*, 370–376.
- [78] G. Taylor, H. H. J. Girault, *J. Electroanal. Chem. interfacial Electrochem.* **1986**, *208*, 179–183.
- [79] C. Gavach, F. Henry, *J. Electroanal. Chem.* **1974**, *54*, 361–370.
- [80] Z. Samec, V. Mareček, J. Weber, *J. Electroanal. Chem.* **1979**, *100*, 841–852.
- [81] E. Smirnov, P. Peljo, M. D. Scanlon, H. H. Girault, *Electrochim. Acta* **2016**, *197*, 362–373.
- [82] A. N. J. Rodgers, S. G. Booth, R. A. W. Dryfe, *Electrochem. commun.* **2014**, *47*, 17–20.
- [83] E. Smirnov, P. Peljo, M. D. Scanlon, H. H. Girault, *ACS Nano* **2015**, *9*, 6565–6575.
- [84] V. Svetličić, N. Ivošević, S. Kovač, V. Žutić, *Bioelectrochemistry* **2001**, *53*, 79–86.
- [85] D. Hellberg, F. Scholz, F. Schauer, W. Weitschies, *Electrochem. commun.* **2002**, *4*, 305–309.
- [86] F. Scholz, D. Hellberg, F. Harnisch, A. Hummel, U. Hasse, *Electrochem. commun.* **2004**, *6*, 929–933.
- [87] N. V. Rees, C. E. Banks, R. G. Compton, *J. Phys. Chem. B* **2004**, *108*, 18391–18394.
- [88] J. Poon, C. Batchelor-McAuley, K. Tschulik, R. G. Compton, C. Damm, D. Omanovic, R. G. Compton, R. G. Compton, G. W. Flynn, S. Park, *Chem. Sci.* **2015**, *6*, 2869–2876.
- [89] H. Wu, Q. Lin, C. Batchelor-McAuley, L. M. Gonçalves, C. F. R. A. C. Lima, R. G. Compton, R. G. Compton, C. Combella, G. W. Flynn, *Analyst* **2016**, *141*, 2696–2703.
- [90] V. Žutić, S. Kovač, J. Tomaić, V. Svetličić, *J. Electroanal.* **1993**, *349*, 173–186.

- [91] R. Tsekov, S. Kovač, V. Žutić, *Langmuir* **1999**, *15*, 5649–5653.
- [92] S. Kovač, V. Svetličić, V. Žutić, in *Colloids Surfaces A Physicochem. Eng. Asp.*, Elsevier, **1999**, pp. 481–489.